

Seismic Waves Scattering Impact through Tunnel Excavation on Adjacent Monuments Subjected to Far Field Earthquakes

Ghobakhloo, E.¹, Pournlak, M.^{2*}, and Razmkhah, A.³

Abstract: The study of the effect of seismic wave scattering has attracted extensive attention in the past couple of decades especially in infrastructures like tunnels. A seismic wave, meeting the tunnel, can generate scattering which, in most cases, may incur damages in adjacent structures. In this study, using Finite Element Method (FEM), the effect of seismic wave scattering in far field has been investigated. The twin tunnels of Shiraz subway system are selected as the case study in this research and three far field seismic waves were chosen for time history analyses. Investigating the normal mode (before tunnel construction) in comparison to the excavation mode (after tunnel construction) enables calculation of the effect of displacement in adjacent structures. The analysis results indicate there is a significant difference between before and after tunnel construction (P -value <0.05). Accordingly, the influence of constructing a tunnel on adjacent surface structures is very important for tunnel design.

Keywords: Scattering of wave; twin tunnel; incident wave direction.

Introduction

When various irregular surfaces like holes or underground structures that are part of the wave change their direction, while the other parts propagate through the medium it is called scattering. This is because of the dissimilarity between the characteristics of the initial medium and the existing underground irregular media. As a primary investigation, Pao et al [1], studied wave diffraction around a cylindrical hole in an infinite medium, where the wave function expansion and the related stress were calculated. Lee et al [2], studied the response of twin tunnels under horizontally polarized wave (SH) propagation in a semi-space, based on the coordinate transformation method. Antonio et al. [3], analyzed a three-dimensional scattering employing cylindrically shaped compound cavities in an elastic formation subject to a broad frequency. Wang et al [4] evaluated the dynamic stress concentration around elliptical cavities in saturated poroelastic soil under harmonic plane waves. Esmaeili et al [5] worked on the dynamic response of the circular lining tunnels to plane harmonic waves.

Lu et al [6] examined the dynamic response of piecewise circular tunnel embedded in poroelastic medium. Zhou et al [7] used a semi-analytical solution in order to explain the scattering of waves in an elastic half-space. Zhou et al [8] then considered an elliptical twin tunnel embedded in a poroelastic medium and analyzed the effect of interaction between the seismic effects of both tunnels. In addition, the behavior of "plane scattering wave" created by cylindrical cavities in poroelastic half-plane has been analyzed by the same authors [9]. Finally, Bin et al [10] studied the dynamic response of a tunnel under water pressure.

In this research, Finite Element modeling (FEM) is employed to investigate the scattering phenomenon. The applied software in this paper is PLAXIS 2D [12] which is based on FEM calculation method and performs the dynamical analysis under far field seismic waves.

Case Study

The case study in this paper is part of Shiraz subway system in which the tunnel goes beneath the ground level, besides the Arg-e-Karimkhan. Arg-e-Karimkhan, named "Arg" in this paper, is located northeast of Shiraz, in Shohada Square, Iran. Its plan shape is rectangular. Arg is Karimkhan Zand's royal palace, in a 12,800 square meter land and has about 4000 square meter area. The four corners of the Arg, have four circular towers that are about 14 meters high and 12 meters in other parts. The outer wall, looks like a fortress walls. Wall thickness at the base of the frustum is 3 m and on top of the wall it becomes 2.8

^{1,3}Department of Civil Engineering, Islamic Azad University-South Tehran Branch, Tehran, IRAN.

² Civil Engineering, Hydraulic Structures, Qom University, Iran. Member of Young Researchers Club-Islamic Azad University South Tehran Branch, Tehran, IRAN.

* Corresponding author; e-mail: mahyar_pournlak@yahoo.com

Note: Discussion is expected before November 1st 2015, and will be published in the "Civil Engineering Dimension" volume 18, number 1, March 2016.

Received 06 December 2014; revised 12 Mei 2015; accepted 17 June 2015

m. Arg foundation and walls are made of stone, while bricks were used to build the rest of the building (Figure 1).

The constructed tunnel is situated below the ground water table and is generally placed in silty gravel and silty clay soil.

The outer and inner diameters of the tunnels are 6.88 and 6 m, respectively. The lining is essentially an assembly of reinforced pre-fabricated concrete segments with 30 cm thickness and 1.4 m width.

The void space (14 cm) between concrete segments and adjacent soil has been injected by cement grout during boring process using Tunnel Boring Machine (TBM). The height of over-burden soil from the tunnels crest to the ground level (Upper Slab) is 19 m (Figure 2). The twin tunnel is parallel to the Zand underpass which is 700 m long and 28 m wide. It includes the upper and lower concrete slabs and in situ reinforced concrete piles as retaining walls. The wall height of Arg is 12 m. Figure 2 illustrates a plot of Arg and Zand underpass.



Figure 1. Arg-e-Karimkhan and the Location

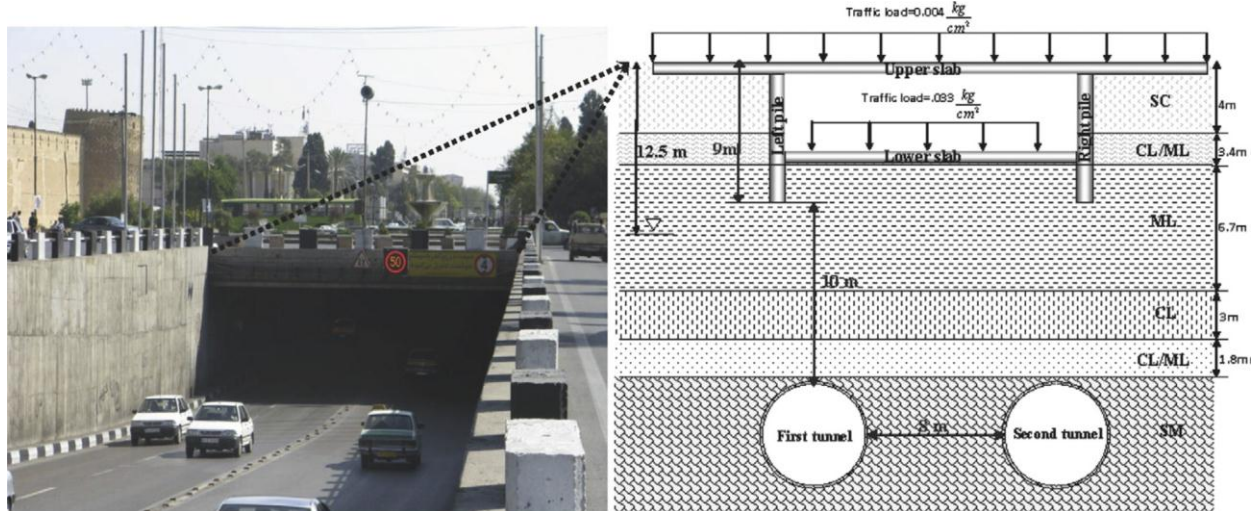


Figure 2. The Relative Position of the Twin Tunnels and Zand Underpass, Arg-e-Karimkhan and Soil Layers [11]

Table 1. Physical and Geotechnical Properties of Soil Layers

No.	Walls Thickness (m)	Soil Type ¹	γ_{sat} (gr/cm ³) ²	γ_{unsat} (gr/cm ³) ³	C_u (Kg/cm ²) ⁴	ϕ_u (°) ⁵	E (Kg/cm ²) ⁶	V^7
1	4	SC	1.09	1.6	0.3	33	325	0.3
2	3.2	CL/ML	2.08	1.7	0.4	29	500	0.25
3	6.7	ML	2.09	1.68	0.1	32	300	0.25
4	3	CL	2.08	1.7	0.2	29	500	0.25
5	1.8	CL/ML	2.09	1.69	0.1	32	500	0.25
6	21.3	SM/ML	2.09	1.77	0.1	29	500	0.25

¹ Based on Unified Soil Classification System

² Saturated Specific Weight

³ Unsaturated Specific Weight

⁴ Cohesion Undrained Soil

⁵ Undrained Inner Friction Angle

⁶ Young Modulus

⁷ Poisson's Ratio

Table 2. Pre-fabricated Segments and Underpass Concrete Properties

Structure	Structural Behavior Model	EA ³ (KN/m)	EI ⁴ (KNm ² /m)	Structure Thickness (m)	W ⁵ (KNm/m)	V
Pre-fabricated Segments	Elastic	9.42e6	7.065e4	0.3	7.5	0.1
Underpass concrete slab	Elastic	2.08e7	1.109e6	0.8	19	0.15
Underpass concrete pile	Elastic	3.12e7	3.744e6	1.2	28	0.15
Right wall of far Arg ¹	Elastic	1.32e7	1.198e7	3.3	49.5	0.3
left wall of far Arg	Elastic	1.12e7	7.317e6	2.8	42	0.3
Right wall of near Arg ²	Elastic	1.28e7	1.092e7	3.2	48	0.3
left wall of near Arg	Elastic	1.32e7	1.198e7	3.3	49.5	0.3

¹The far Wall of the Arg in relation to the twin tunnels is called "Far Arg"

²The close Wall of the Arg to the twin tunnels is called "Near Arg" (Therefore distance between far Arg² and near Arg from left tunnel wall is 133 m and 33 m respectively.)

³ Axial Rigidity

⁴ Flexural (Bending) Rigidity

⁵ Structural Weight per meter

Geology and Geotechnics

The geological profile of the case study includes 6 layers of soil with various thicknesses and properties. Soils are organized with respect to Unified Soil Classification System [11]. The level of the

ground water table is 6.5 m below the tunnels crest. The soil properties and the construction material used in the Arg as well as the tunnel and the underpass properties are mentioned in Table 1 and 2, respectively [11].

Scattering Analysis

The modeling is based on the plane strain condition with proper 15 triangular mesh types. The sensitivity analysis is carried out for the boundaries and the meshes. The final dimensions and meshes are demonstrated in Figure 3. Boundaries are selected properly, in order to prevent the wave reflection. In refine mesh processes, the mesh dimensions are reduced due to the sensitivity around the tunnel, Arg and Zand underpass [12]. In the implementation of earthquake in the soil areas (like this case), in order to avoid reflection of waves and appearance of extra stress on the structure, the boundaries have been applied away from the main structure. Indeed, Layer 6 is the bedrock (layer), from which the seismic wave has been propagated. Absorbent boundaries are assumed at the bottom and both sides of the model. This boundary at the bottom is located in the bedrock and in both sides and is far enough from the tunnel structure and the Arg. Then the wave reflection would not happen. Sensitivity analysis has been performed on these distances and the resulting figure is obtained (Figure 3).

According to the soil type of the case study area, special stations of Chichi, Kobe, and Northridge time history seismic records are selected for far field studies (Figure 4).

In accordance with Iran standard No. 2800 [13], Shiraz area has a relatively high risk of earthquake occurrence and the maximum earthquake acceleration should be scaled to 0.3g. The proper time for accelerographs is 20 seconds in which it is more critical and the maximum response can be achieved.

In the dynamic modeling, the soil type was considered Mohr-Coulomb, with undrained behavior and Rayleigh-damping (α and β) of 0.01.

Analyzing the Behavior of Arg-e-Karimkhan

In order to analyze Arg, far field accelerographs are applied to the structure at different wave directions in degrees. For studying the scattering phenomenon, the control points in the structure farther from the tunnel (A, B) and the Arg nearer to the tunnel (C, D) are illustrated above the structure on earth. The differential displacement for each structure is investigated at various directions by measuring the difference between the top and bottom displacements of the modelled structure as shown in Figure 3. The maximum differential seismic displacements before and after tunnel excavation within earthquake duration, will be evaluated with the displacement before/after excavation.

$$\begin{aligned}
 U &= U_{TOP} - U_{BOT} \\
 U &= U_A - U_B \quad \text{for Far Arg} \\
 U &= U_C - U_D \quad \text{for Near Arg}
 \end{aligned}
 \tag{1}$$

The total displacement in both structures subject to far field seismic waves of Kobe, Northridge and Chichi directed with the sample angle 37°(and also 0° and 45° directions), are shown in Figure 5, 6, 7, 8, 9, and 10, respectively. These angles are measured from horizontal datum and have been considered in the analysis.

The purpose of this research is to analyze the effect of tunnel excavation on Arg. Regarding the explained geometry in the text, the thickness of Arg wall in “Arg far wall” and “Arg near wall”, is not equal, but the materials are the same. Meanwhile,

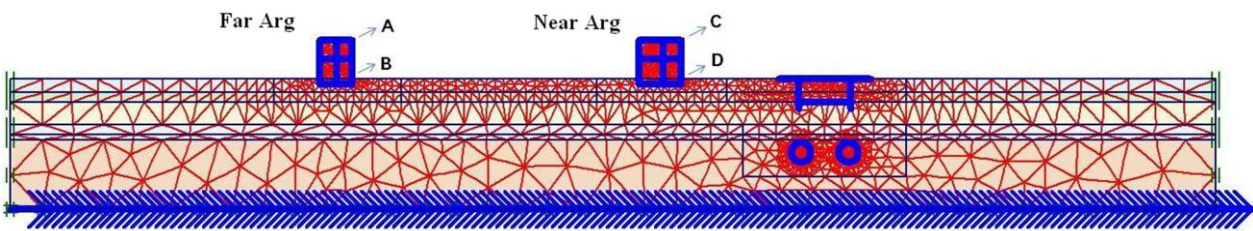


Figure 3. The Geometrical Model of the Case Study Land

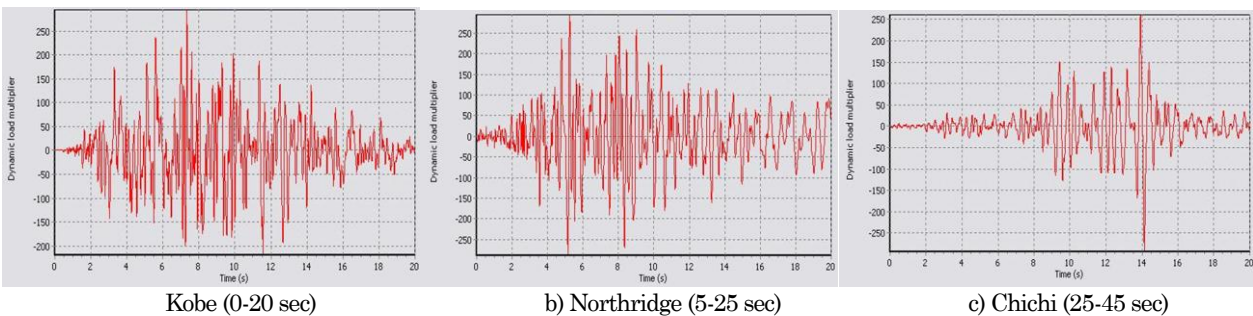


Figure 4. Acceleration of Far Field Earthquake

based on this analysis, more results can be obtained from the structures regarding the distance from the tunnel and the thickness concurrently.

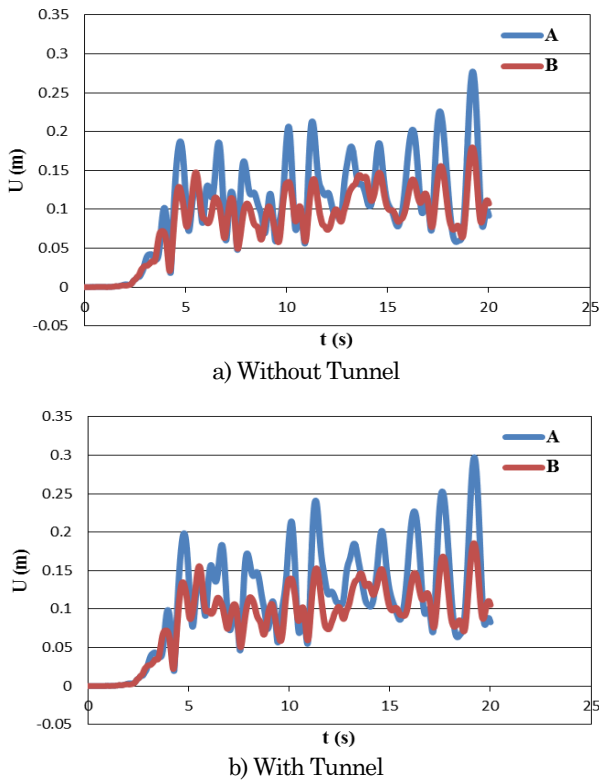


Figure 5. The Total Displacement Evaluation in the Far Arg from the Tunnel under the Kobe Earthquake in 37 Degree Direction

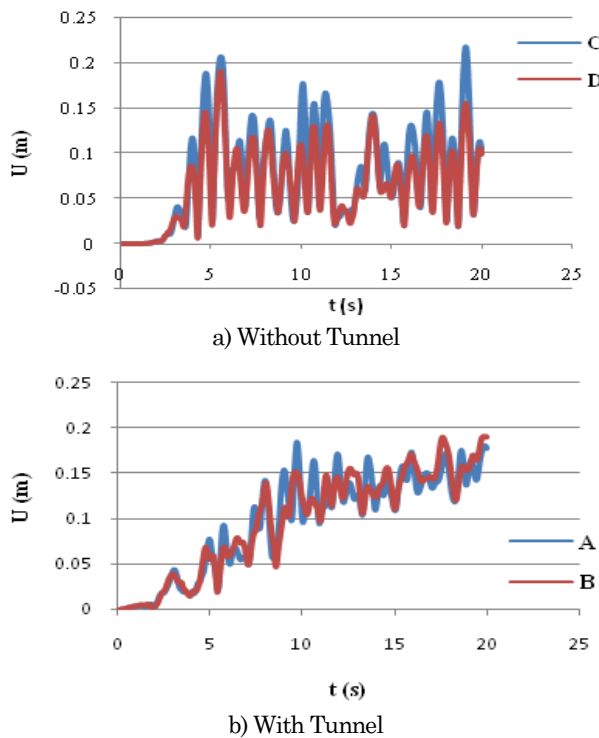


Figure 6. The Total Displacement Evaluation in the Near Arg from the Tunnel under the Kobe Earthquake in 37 Degree Direction

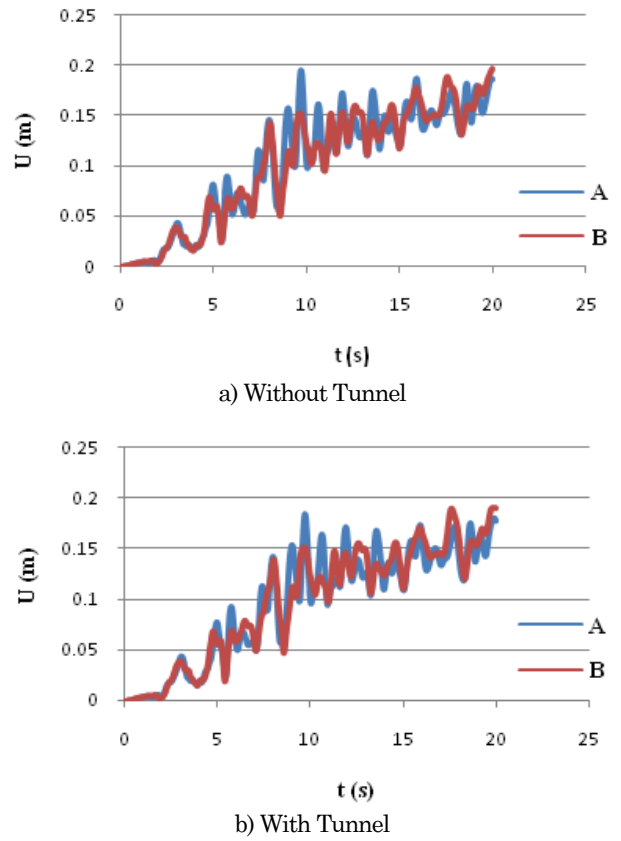


Figure 7. The Total Displacement Evaluation in the Far Arg from the Tunnel under the Northridge Earthquake in 37 Degree Direction

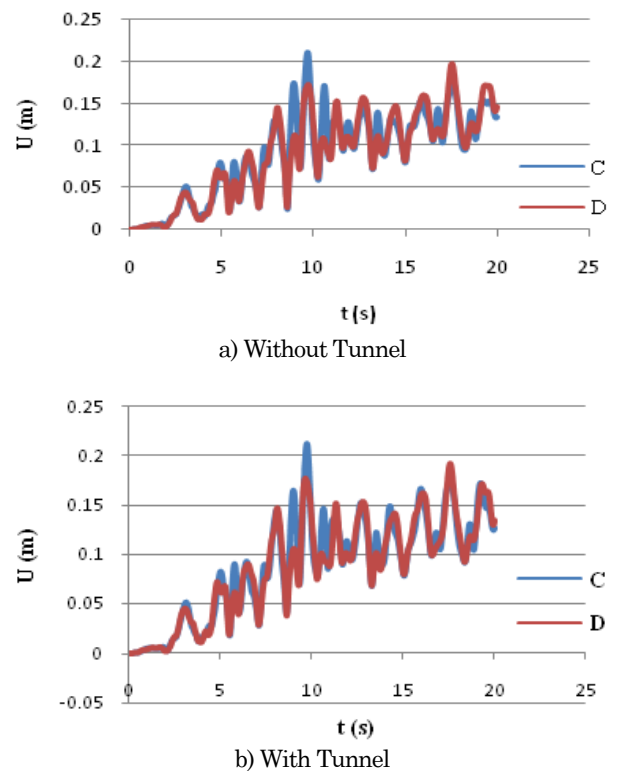


Figure 8. The Total Displacement Evaluation in the Near Arg from the Tunnel under the Northridge Earthquake in 37 Degree Direction

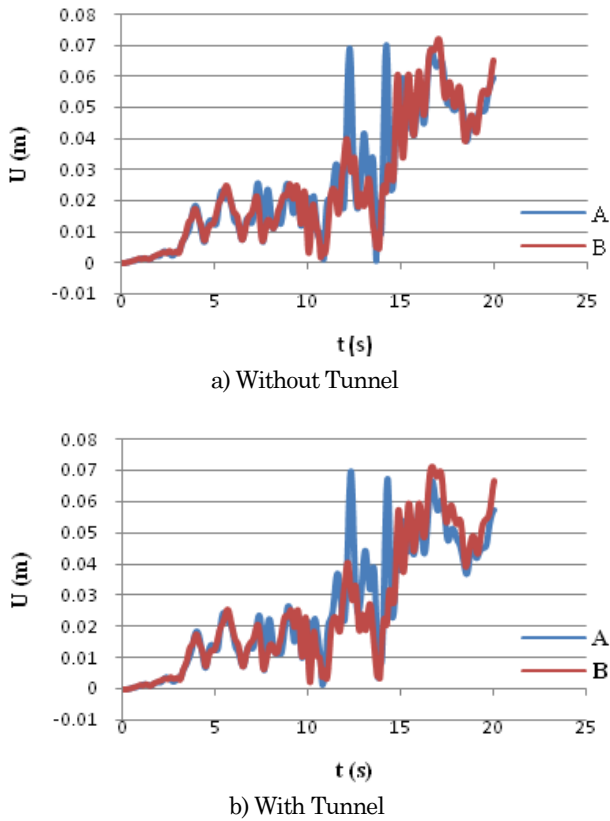


Figure 9. The Total Displacement Evaluation in the Far Arg from the Tunnel under the Chichi Earthquake in 37 Degree Direction

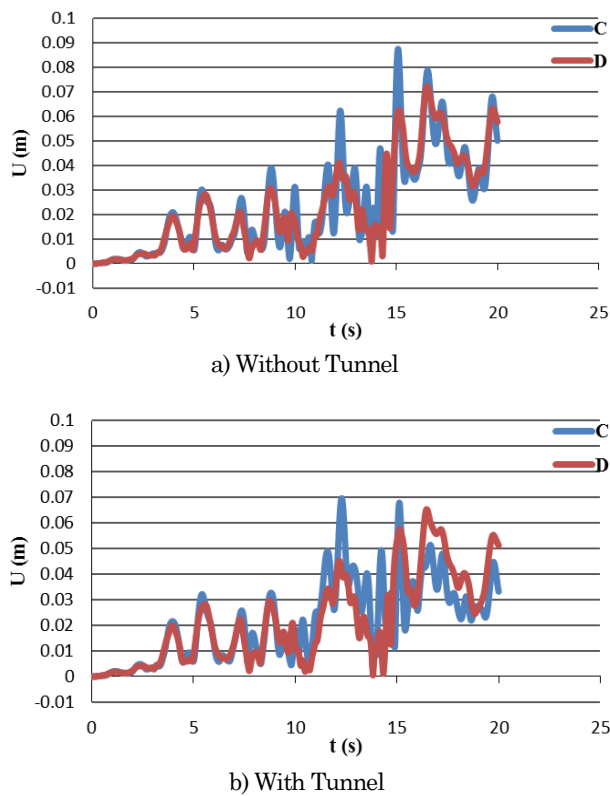


Figure 10. The Total Displacement Evaluation in the Near Arg from the Tunnel under the Chichi Earthquake in 37 Degree Direction

The corresponding scattering quantities due to far field seismic waves were shown in Tables 3 and 4. Using SPSS software and Mann-Whitney test [14], differential displacement amplitudes in Arg with tunnel and without tunnel construction are compared.

Conclusions

The effect of seismic wave scattering was studied considering the construction of the tunnel under far field earthquakes specifically for Arg-e-Karimkhan, Iran where the subway’s tunnel passes beneath the Zand underpass and beside Arg. Utilizing the Plaxis software and based on FEM analysis, the simulation of the mentioned area and dynamic analysis of far field seismic waves have been carried out.

1. According to Table 3, the maximum scattering percentage related to the far field study is 14.12% for Kobe earthquake with a direction angle of 37°, for Chichi earthquake, is -7.09% with a direction angle of 0°, and for Northridge earthquake is -4.03%, at 0°. As was shown in Table 3 and 4, far and near Arg has been analyzed with respect to the tectonic and Shiraz field considerations. Wave directions for all waves are the same and vary from 0° to 45° relative to horizon. Regarding Eq. 1, the displacement has been measured in two conditions of before and after excavation of the tunnels. The difference between these two conditions has been taken as scattering percentage. In some earthquakes, this percentage appears less than zero. This shows, under special circumstances, the tunnel excavation has a reverse effect on the maximum differential displacement of the structure.
2. According to Table 4, the maximum scattering percentage related to the far field study directed at an angle of 45°, near Arg is -13.11% for Kobe earthquake, at 37° is 25.60% for Chichi earthquake, and at 45° is -12.14% for Northridge earthquake.
3. The maximum P-value measure in the far field earthquake has happened for “Arg far wall” with the value of 0.981 and for “Arg near wall” is 0.76 under the Kobe earthquake at 0° degree.
4. In some far field earthquakes, the effect of tunnel acts reversely and the percentage of scattering happens appears to be negative. These measures show that excavation of Shiraz tunnel causes lower drift in the Arg. These measures highly depend on the earthquake frequency, the kind of structures, the distance between the structures and tunnel, the dimensions, and the weight of the structure.

Table 3. The Scattering in the Far Arg

Earthquake	Wave direction (degree)	Maximum differential seismic displacements after tunnel excavation (m)	Maximum differential seismic displacements before tunnel excavation (m)	Percentage of scattering (%)	P-value
Chichi	0	0.0485	0.0522	-7.09	0.077
	37	0.0449	0.0463	-3.02	0.00
	45	0.0453	0.0466	-2.79	0.00
Northridge	0	0.0619	0.0645	-4.03	0.913
	37	0.0480	0.0487	-1.44	0.066
	45	0.0449	0.0467	-3.85	0.005
Kobe	0	0.1314	0.1294	1.55	0.981
	37	0.1123	0.0984	14.12	0.013
	45	0.1051	0.0921	14.11	0.006

Table 4. The Scattering in the Near Arg

Earthquake	Wave direction (degree)	Maximum differential seismic displacements after tunnel excavation (m)	Maximum differential seismic displacements before tunnel excavation (m)	Percentage of scattering (%)	P-value
Chichi	0	0.0764	0.0635	20.32	0.00
	37	0.0417	0.0332	25.60	0.619
	45	0.0352	0.0328	7.32	0.00
Northridge	0	0.0651	0.0650	0.15	0.002
	37	0.0599	0.0655	-8.55	0.659
	45	0.0557	0.0634	-12.14	0.485
Kobe	0	0.0932	0.0928	0.43	0.76
	37	0.0787	0.0898	-12.36	0.607
	45	0.0808	0.0930	-13.11	0.702

5. The analysis results show there is significant difference between before and after tunnel construction (P-value<0.05). Accordingly, the influence of construction of a tunnel on adjacent surface structures is very important for tunnel design.

References

- Pao, H.Y. and Mow, C.C., *The Diffraction of Elastic Waves and Dynamic Stress Concentrations*, Rand Corporation, USA, 1971.
- Lee, V.W. and Trifunac, M.D., Response of Tunnels to Incident SH-Waves, *J. Eng. Mech. Div ASCE*, 108, 1982, pp. 1-17.
- Antonio, J. and Tadeu, A., 3D Scattering by Multiple Cylindrical Cavities Buried in an Elastic Formation, *Eur. J. Mech. A/Solids*, 20, 2001, pp. 367-383.
- Wang, J.H., Zhou, X.L., and Lu, J.F., Dynamic Stress Concentration around Elliptic Cavities in Saturated Poroelastic Soil under Harmonic Plane Waves, *International Journal of Solids and Structures*, 42, 2005, pp. 4295-4310.
- Esmaili, M., Vahdani, S., and Noorzad, A., Dynamic Response of Lined Circular Tunnel to Plane Harmonic Waves, *Tunnelling and Underground Space Technology*, 21, 2006, pp. 511-519.
- Lu, J.F., Jeng, D.S., and Lee, T.L., Dynamic Response of a Piecewise Circular Tunnel Embedded in a Poroelastic Medium, *Soil Dynamics and Earthquake Engineering*, 27, 2007, pp.875-891.
- Zhou, X.L., Jiang, L.F., and Wang, J.H., Scattering of Plane Wave by Circular-Arc Alluvial Valley in a Poroelastic Half-Space, *Journal of Sound and Vibration*, 318, 2008, pp. 1024-1049.
- Zhou, X.L., Wang, J.H., and Jiang, L.F., Dynamic Response of a Pair of Elliptic Tunnels Embedded in a Poroelastic Medium, *Journal of Sound and Vibration*, 325, 2009, pp. 816-834.
- Jiang, L.F., Zhou, X.L., and Wang, J.H., Scattering of a Plane Wave by a Lined Cylindrical Cavity in a Poroelastic Half-Plane, *Computers and Geotechnics*, 36, 2009, pp. 773-786.
- Bin, L., Kang He, X., and Xiaohu, L., Dynamic Response of a Partially Sealed Tunnel in Porous Rock under Inner Water Pressure, *Tunnelling and Underground Space Technology*, 25, 2010, pp. 407-414.
- Afifipour, M., Shrifzadeh, M., Shahriar, K., and Jamshidi, H., Interaction of Twin Tunnels and Shallow Foundation at Zand Underpass, Shiraz Metro, Iran, *Tunneling and Underground Space Technology*, 26, 2011, pp. 356-363.
- Brinkgreve, R.B.J. and Broere, W., *Plaxis Dynamics Manual* (ver 8.5), Delft University of Technology and Plaxis b.v., Netherlands, 2006.

13. Standard No. 2800–05 (3rd Edition), *Iranian Code of Practice for Seismic Resistant Design of Building*, Building and Housing Research Center, 2005. (In Persian).
14. Mann, H.B. and Whitney, D.R., On a Test of Whether One of Two Random Variables is Stochastically Larger than The Other, *Annals of Mathematical Statistics*, 18(1), 1947, pp. 50–60.